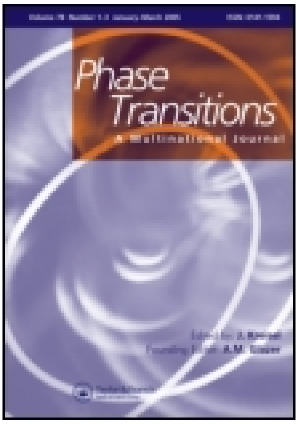

Phase Transitions: A Multinational Journal

Publication details, including instructions for authors and subscription information:
http://www.tandfonline.com/loi/gpht20

Physical properties of a bent-core nematic liquid crystal and its mixtures with calamitic molecules

Á. Buka [a], N. Éber [a], K. Fodor-Csorba [a], A. Jákli [b] & P. Salamon [a]

[a] Institute for Solid State Physics and Optics, Wigner Research Centre for Physics, Hungarian Academy of Sciences, P.O. Box 49, H-1525 Budapest, Hungary

[b] Liquid Crystal Institute, Kent State University, Kent, OH 44242, USA

Version of record first published: 07 Jun 2012.

To cite this article: Á. Buka , N. Éber , K. Fodor-Csorba , A. Jákli & P. Salamon (2012): Physical properties of a bent-core nematic liquid crystal and its mixtures with calamitic molecules, Phase Transitions: A Multinational Journal, 85:10, 872-887

To link to this article: http://dx.doi.org/10.1080/01411594.2012.689834

Phase Transitions
Vol. 85, No. 10, October 2012, 872–887

Physical properties of a bent-core nematic liquid crystal and its mixtures with calamitic molecules

Á. Buka[a]*, N. Éber[a], K. Fodor-Csorba[a], A. Jákli[b] and P. Salamon[a]

[a]*Institute for Solid State Physics and Optics, Wigner Research Centre for Physics, Hungarian Academy of Sciences, P.O. Box 49, H-1525 Budapest, Hungary;* [b]*Liquid Crystal Institute, Kent State University, Kent, OH 44242, USA*

(*Received 27 March 2012; final version received 26 April 2012*)

This article summarizes the results obtained by various experimental methods on the physical properties of a bent-core nematic liquid crystal 4-chloro-1,3-phenylene bis-4-[4′-(9-decenyloxy) benzoyloxy] benzoate (**ClPbis10BB**). The material exhibits unusual properties in all aspects tested. Its bend flexoelectric coefficient is 1000 times larger than in calamitics; it is viscoelastic with a large, shear-rate-dependent viscosity. Its bend and twist elastic constants are abnormally low; thus the nematic phase can be rendered to be a blue fog phase with a small amount of chiral dopant. It shows very high flow birefringence and unusually small leading Landau coefficient. It has two types of isotropic phases; at lower temperature it is probably tetrahedratic that can be transferred into the nematic phase with magnetic field. **ClPbis10BB** has a frequency-dependent conductivity anisotropy which is characterized by a double sign inversion. It exhibits various electroconvection (EC) patterns which are currently not understood in the frame of the standard theory of EC.

Keywords: bent-core nematic liquid crystal; flexoelectricity; dielectric spectroscopy; elastic constant; electroconvection; flow birefringence

1. Introduction

Bent-core (BC) mesogens represent a novel class of thermotropic liquid crystals (LCs) which have become targets of extensive studies in the last decade [1]. Due to the bent shape, in contrast to calamitic LCs, the closest packing of such molecules can be polar. Therefore, they can form a number of new mesophases besides the regular ones known for calamitics. To date, most of the research effort has focused on BC smectic structures (‘banana’ phases [2] identified as $B_1, \ldots, B_8$). The polar packing in such banana phases may lead to ferroelectric or anti-ferroelectric ordering even if the constituent molecules are achiral [3,4]. Theoretical studies [5–9] predicted the potential existence of new liquid phases exhibiting purely orientational order (i.e., varieties of nematic phases). These include biaxial phases [5,6], an orientationally ordered but optically isotropic phase [7,8], and even spontaneously chiral and polar liquid phases [9] which are all theoretically possible due to the bent shape of molecules though have not yet been unambiguously identified among synthesized compounds. Nematic (uniaxial) phases have been found to be rather

---

*Corresponding author. Email: buka.agnes@wigner.mta.hu

ISSN 0141–1594 print/ISSN 1029–0338 online

http://dx.doi.org/10.1080/01411594.2012.689834
http://www.tandfonline.com

uncommon in BC compounds, though recently a number of new BC substances with nematic phases have also been synthesized [10–14]. Unfortunately most of them exhibit the nematic phase at rather high temperatures (well over 100°C), causing challenges in the detailed investigation of their physical properties.

In search for compounds with a lower clearing point, we have synthesized some BC benzoyloxy benzoate derivatives [15]. Some of these compounds exhibit a monotropic nematic (N) phase in cooling at relatively low temperatures (below 80°C). One member of the family, 4-chloro-1,3-phenylene bis-4-[4′-(9-decenyloxy) benzoyloxy] benzoate (**ClPbis10BB**), has turned to be especially popular, becoming a kind of reference BC nematic. It has been investigated by several research groups with complementary methods; various physical properties have been determined [16–18], pointing out significant differences compared to those of calamitic nematics and initiating further studies on other BC nematics.

In this article, we summarize the results of available measurements in order to provide a detailed characterization of the compound(s) as much as currently possible. We address the synthesis, the mesomorphic properties, miscibility, rheological, structural, and NMR studies. We report on dielectric, flexoelectric and viscoelastic properties as well as on peculiarities in electric field induced patterns. Finally, we close this article with some conclusions.

2. Synthesis, phase behavior, and miscibility

2.1. *Synthesis*

The synthetic route of the benzoyloxy benzoate series is depicted in Figure 1. The synthesis starts from the 4-hydroxy benzoic acid (**1**). The phenolic part of the molecule had to be protected. Hence an ethoxy-carbonyloxy group was chosen and the compound **2** was isolated. After activating the carboxyl group (compound **3**), it was connected to the differently substituted resorcinol derivatives (**4**) leading to compound **5**. After decoupling the protecting group, a three-ring-containing intermediate (**6**) was obtained. This key intermediate was connected to the unsaturated terminal-chain-containing compound **7** leading to the formation of the final product (**8**). The X, Y, and Z symbols could mean either hydrogen, chlorine or methyl group; the terminal chains were decenyloxy or undecenyloxy groups. The properties of the differently substituted resorcinol derivatives are summarized in Table 1.

2.2. *Phase behavior*

The electron withdrawing chlorine atom in the central benzene ring, due to its relative bulkiness, can suppress the molecules locking into smectic layers, thus favoring a nematic phase. In addition, because of the unsaturated tails, these compounds exhibited the nematic phase at a lower temperature range than their saturated analogs.

Magnetic birefringence and dynamic light scattering (DLS) measurements of orientational order parameter fluctuations at the isotropic–nematic phase transition of a BC LC revealed a pretransitional temperature dependence consistent with the standard Landau-deGennes mean field theory. However, the transition in the BC compound is more weakly first order, the supercooling limit (T^*) is only 0.4°C below the clearing point, the leading Landau coefficient is 30 times lower, the viscosity associated with nematic order fluctuations is 10 times higher, and the density change is 10 times lower, than typically

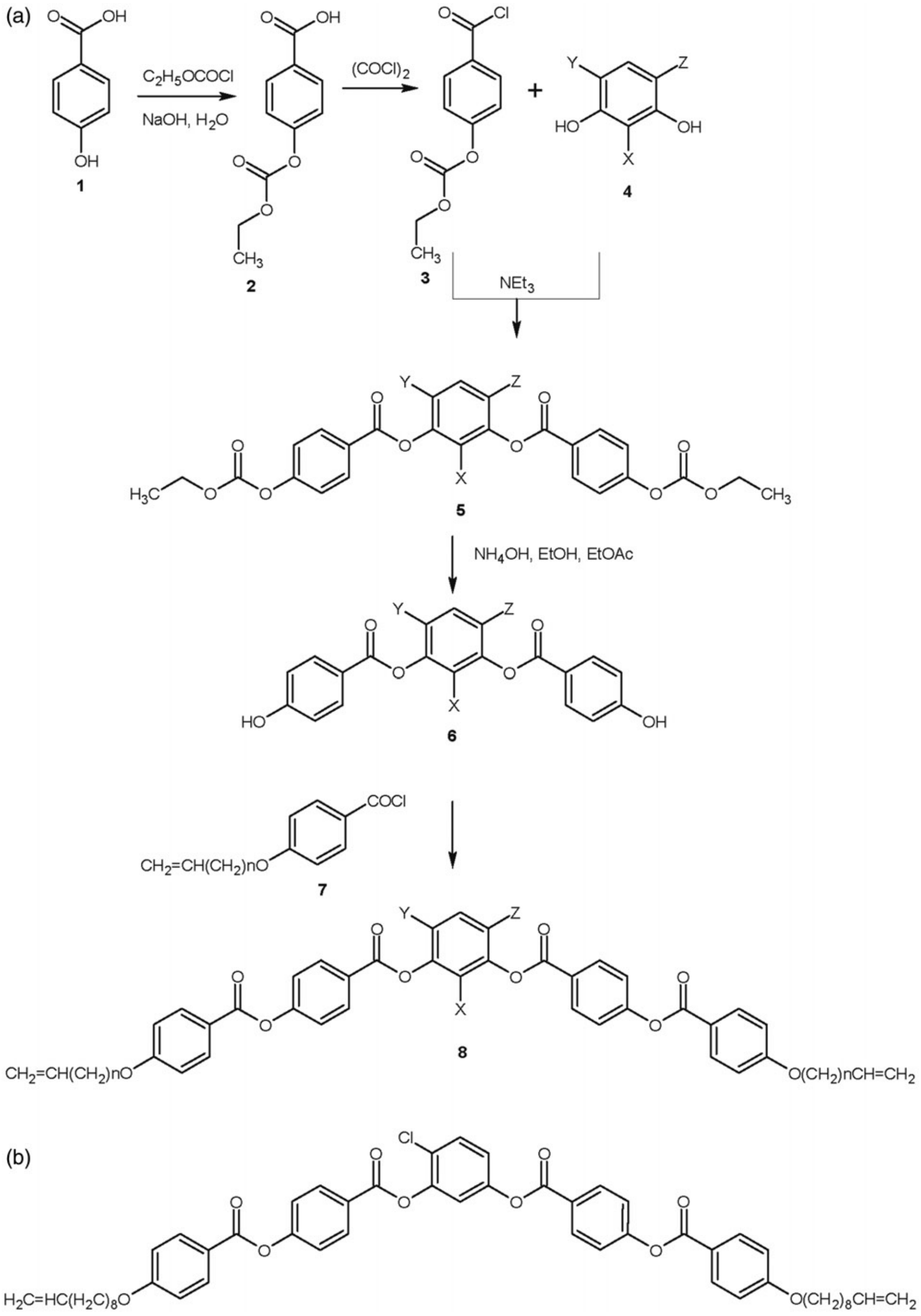

Figure 1. (a) Synthetic route for the preparation of benzoyloxy benzoate derivatives. (b) Schematic chemical structure of the banana nematic **ClPbis10BB**.

observed in calamitic rod-shaped LCs [17]. An experimental study of the heat capacity, mass density, magnetic-field-induced optical birefringence, linewidth and intensity of scattered light, and the viscosities associated with nematic order parameter fluctuations and fluid flow performed on **ClPbis10BB** above its clearing point temperature revealed a

Table 1. Phase behavior of the resorcinol derivatives.

Terminal chain	X	Y	Z	Phase behavior	Abbreviation
Decenyloxy-	H	H	H	Cr 97.0 Iso	**Pbis10BB**
Undecenyloxy-	H	H	H	Cr (98.0 B2)101.0 Iso	**Pbis11BB**
Decenyloxy-	H	Cl	H	Cr (47.0 SmC) 67.6 N 73.5 Iso	**ClPbis10BB**
Undecenyloxy-	H	Cl	H	Cr (44.0 SmC) 74.0 N 81.0 Iso	**ClPbis11BB**
Decenyloxy-	CH_3	H	H	Cr 110.0 Iso	**MePbis10BB**
Undecenyloxy-	CH_3	H	H	Cr 112.0 Iso	**MePbis11BB**
Decenyloxy-	D	Cl	D	Cr (47.0 SmC) 67.6 N 73.5 Iso	**ClPbis10BB-dx**
Undecenyloxy-	D	Cl	D	Cr (44.0 SmC) 74.0 N 81.0 Iso	**ClPbis11BB-dx**

transition between two optically isotropic phases [19] that is consistent with recent theoretical predictions of an isotropic to tetrahedratic phase transition [8,20].

Measurements of magnetic-field-induced nematic order using the 31 T solenoid at the National High Magnetic Field Laboratory (USA), demonstrated a first-order transition to the nematic phase at temperatures less than 1°C above the clearing point [21]. The critical magnetic field, at which this occurs, increases with temperature. These results represent the first observations of a magnetic-field-induced transition in a thermotropic LC, and were discussed within the context of both Maier-Saupe and Landau-de Gennes mean-field models for the nematic–isotropic transition. It was also found that this and other BC liquid crystalline materials show exceptionally large intrinsic flow birefringence in their isotropic liquid phase (Figure 2). This effect is more than 100 times larger than typical values measured for low molecular weight LC [22]. The specific flow birefringence (i.e., normalized by the flow viscosity) is an order of magnitude larger than in side-chain polymeric as well as in low molecular weight LCs. All the above unusual phase behaviors can be consistently explained by assuming that the optically isotropic phase is composed of microscopic complexes or 'clusters' of BC molecules. This assumption was verified by small angle X-ray measurements to be described below.

2.3. *Additional features*

Binary mixtures of our bent-shape material **ClPbis10BB** with rod-shape molecules 4-n-octyloxyphenyl 4-n-hexyloxybenzoate (**6OO8**) [23] similar to one arm of **ClPbis10BB**, form nematic and a biaxial smectic phase in a wide temperature range including the room temperature. Based on polarizing microscopy and small angle X-ray scattering (SAXS) measurements it was shown that the biaxial smectic phase has an anticlinic director structure (SmC_A) [24]. The tilt plane of the molecules could easily be switched by an electric field, providing a change of the birefringent color without the rotation of the optical axis with sub-millisecond switching times. The room temperature operation and the uniform alignment offer their immediate applications as linear phase modulators or fast displays.

In **ClPbis10BB** doped with a high twisting power chiral material **BDH-1281**, an induction of the blue phase III (BPIII) [25] at relatively low temperatures in a wide (over 20°C) temperature range was found [26]. It was shown that the pitch decreases with increasing chiral dopant ratio and easily reaches the ultraviolet wavelength, so that a completely dark texture is obtained between crossed polarizers. Electro-optical switching

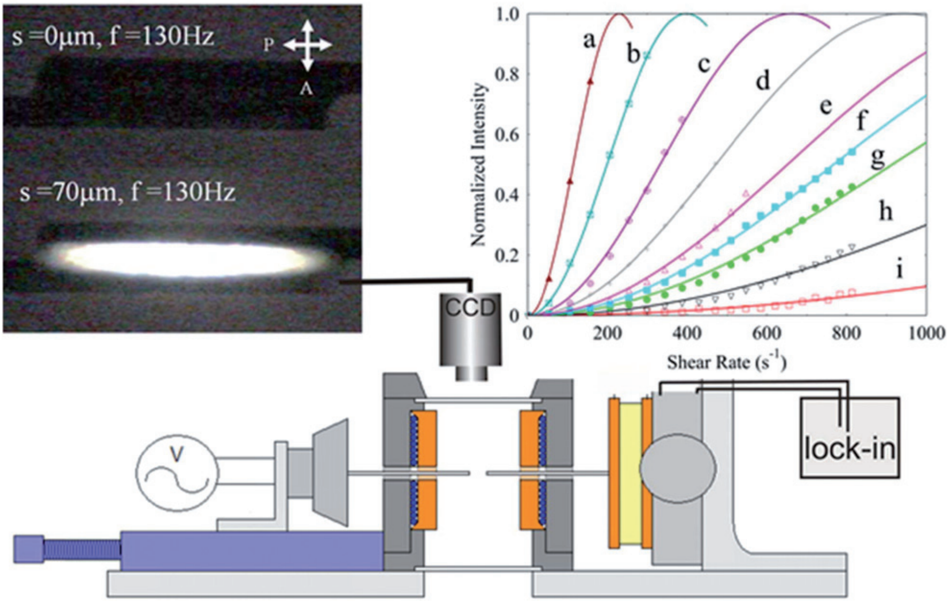

Figure 2. Illustration of the shear induced birefringence of **ClPbis10BB** measured between crossed polarizers in the isotropic phase. Lower part: schematics of the experimental setup; upper left: polarizing microscope pictures of the material at 76.3°C between the actuating and sensing rods of the nl-rheometer without shear (top) and with shear with $\dot{\gamma} \sim 570\,\mathrm{s}^{-1}$(bottom). Upper right: graph of the measured and fitted normalized transmitted intensity *vs.* shear rate at (a) 74.7°C, (b) 75.2°C, (c) 76.2°C, (d) 77.2°C, (e) 78.2°C, (f) 79.2°C, (g) 80.2°C, (h) 82.2°C, and (i) 87.5°C above the nematic phase.

was achieved in a switching time range of a few to a few tens of milliseconds. It was proposed that the stabilization of BPIII is due to the broad-temperature-range smectic nano-clusters that inhibit the long-range order of the double-twisted helical structures, and also suppress the separation of chiral dopants from the mixture.

3. NMR studies

For the better understanding of the conformational changes in the banana phases, two BC materials were investigated by 2H NMR method. For this purpose, selectively deuterated isotopomers of **ClPbis11BB-d3** and of **Pbis11BB-d4** were synthesized. The **ClPbis11BB-d3** exhibits nematic phase, while the **Pbis11BB-d4** has B_2 phase. The BC materials were dissolved in a nematic host media **Phase IV** and **ZLI-1167**, which should mimic the environment of the molecules in their own mesophases, avoiding the problems of sample alignment in magnetic field. Two parent deuterated molecules: **ClPbisB-d3** and **PbisB-d4** containing only the central part of the BC materials were also used in these studies. These studies made clear that only a limited number of conformations is compatible with experimental data, and they differ considerably from those conformations calculated theoretically *in vacuo*. These results indicate the strong influence of the liquid crystalline environment on the conformations which can exist in the banana phases. No significant difference was found between the chlorinated and non-chlorinated derivatives, suggesting that the chlorine does not induce too much change in the conformational equilibrium [27].

For the further detailed studies on the deuterium labeled **ClPbis11BB**, selectively deuterated isotopomers were synthesized. These compounds have the labeling either on the central ring (**ClPbis11BB-C-d3**) or on the symmetrical two inner rings (**ClPbis11BB-I-d4**) of the wings and finally labeling was introduced to the outer rings (**ClPbis11BB-O-d4**). For these labeled compounds a new synthetic procedure has been developed. The 2H NMR data were interpreted assuming that the central aromatic ring is oriented perpendicular to the external magnetic field [28]. This assumption seems, however, to be inconsistent with Freedericksz-transition measurements indicating a positive diamagnetic anisotropy [29]. The mesophase is assumed to be uniaxial, the orientational order parameter was determined: S_2 ranges between 0.32 and 0.52. It is typical for the nematic LCs. The values for the orientation of the four lateral rings showed that the inner rings are more ordered than the outer rings. The average conformation of the wing close to the chlorine atom was different from that of the other wing [30,31].

4. Dielectric properties

The key electric properties determining the behavior of a compound in an electric field are the dielectric permittivity and the electrical conductivity. They have been measured for **ClPbis10BB**, as well as for its mixtures with the calamitic compound **6OO8**, using dielectric spectroscopy in the $100\,\mathrm{Hz} < f < 10\,\mathrm{MHz}$ frequency (f) range [32]. The technique yields information on the frequency dependence of the complex dielectric permittivity, $\varepsilon^*(f) = \varepsilon'(f) - i\varepsilon''(f)$, where the real part ($\varepsilon'$) corresponds to the dielectric permittivity, while the electrical conductivity may be obtained from the imaginary part (the dielectric loss) via the relation $\varepsilon'' = 2\pi f \sigma$. Measurements have been performed using sandwich cells with gold-plated electrodes; the LC in the cell was oriented by a magnetic field either parallel or normal to the electrodes, thus both $\varepsilon^*_\perp$ and $\varepsilon^*_{||}$ could be obtained.

Measurements showed that both the pure compounds and the mixtures have a negative dielectric anisotropy ($\varepsilon_a = \varepsilon_{||} - \varepsilon_\perp < 0$), but the dielectric relaxations in the nematic phase of **ClPbis10BB** have some distinctive character compared to those of typical calamitic nematics. Figure 3 shows the frequency dependence of the dielectric loss for the two measuring geometries. Two dispersions can clearly be identified in the parallel and one in the perpendicular component, however, one more dispersion has to be present at higher frequencies in each component. This implies that the BC nematic exhibits more dispersions than usual calamitics. In addition, the relaxation frequencies are found to be substantially

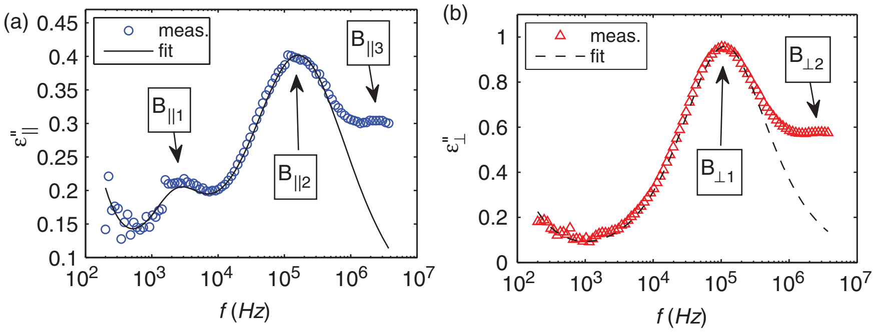

Figure 3. Dielectric spectra of **ClPbis10BB**. (a) Parallel component and (b) perpendicular component.

lower than those of other nematics; the lowest one is in the parallel component just at a few kHz. As a consequence of the low frequency dispersion, the frequency dependence of the conductivity anisotropy is quite unusual: σ_a changes sign twice in the $10\,\text{Hz} < f < 100\,\text{kHz}$ frequency range. To explore the relation between the observed dispersions and molecular motions one would still need further experimental and theoretical studies. Especially it is unclear whether the low f relaxation can be associated with dynamics of individual molecules or it should be the consequence of a collective mode of the smectic clusters present in the banana nematic.

In the dielectric spectra of the binary mixtures of the BC **ClPbis10BB** and the calamitic **6OO8** it was found that the lowest frequency relaxation mode disappears at about 50 wt% of the **6OO8** concentration in accordance with the disappearance of the smectic clusters in the mixtures.

5. Flexoelectricity

Flexoelectricity is a LC specific phenomenon whose concept was introduced by Meyer [33]. Its essence is that splay or bend deformations of the director **n** induce a flexoelectric polarization $\mathbf{P}_{fl} = e_1\mathbf{n}(\nabla\mathbf{n}) + e_3(\nabla \times \mathbf{n}) \times \mathbf{n}$ [33,34].

The magnitude of the effect is characterized by two (splay and bend) flexoelectric coefficients, e_1 and e_3, respectively. Microscopically two mechanisms contribute to flexoelectricity, a dipolar and a quadrupolar one. The dipolar contribution comes from the partial polar ordering of the dipole moments of pear- or banana-shaped molecules in the splay-bend distorted environment [35–37]. The quadrupolar contribution, on the contrary, does not require shape asymmetry of molecules. It is obvious, that the large kink angle of the BC molecules makes them ideal candidates for a compound with large dipolar contribution to e_3.

A new method based on an oscillatory mechanical bending of a planar aligned LC layer sandwiched between flexible electrode plates was first applied to the compound **ClPbis10BB** to measure e_3 [18]. From the measured current $|e_3|$ could be calculated. Its temperature dependence is shown in Figure 4(a). A big jump can be seen at the isotropic-to-nematic phase transition temperature T_{NI} indicating that this transition is of first order. The maximum response, $|e_3| \approx 35\,\text{nC}\,\text{m}^{-1}$, was detected a few degrees below T_{NI}, then it fell back to almost zero when crystallization occurred. For comparison, the temperature dependence of e_3 of a well-known calamitic nematic, 4-cyano-4′-n-pentyl-biphenyl (**5CB**) is

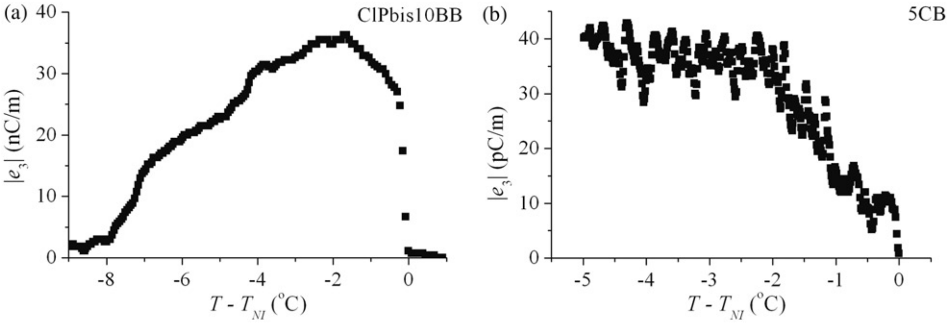

Figure 4. Magnitude of the flexoelectric coefficient $|e_3|$ *vs.* the temperature deviation from the nematic-isotropic phase transition for (a) **ClPbis10PP** and for (b) **5CB**.

shown in Figure 4(b). It indicates a rather gradual increase and three orders of magnitude lower values when passing T_{NI} matching roughly with those obtained for **5CB** by electro-optical methods [38,39].

The converse effect has been detected in **ClPbis10BB** sandwiched between flexible substrates, but only at a voltage above a threshold value, where a bending of the substrates could be observed by an interferometric technique [40,41]. The flexoelectric coupling coefficient e_3 calculated from the induced curvature matched the giant value obtained from the direct measurements using the flexing technique mentioned above. Another manifestation of converse flexoelectricity, the optically detectable electric-field-induced reorientation using hybrid-aligned nematics (HAN cell) [38,39,42–49] did not work for **ClPbis10BB**, as the resulting alignment was almost planar even near the homeotropic surface due to a high internal DC bias voltage $U_e = -\frac{(e_1+e_3)}{2\varepsilon_a\varepsilon_a}\ln\frac{\varepsilon_{\parallel}}{\varepsilon_{\perp}}$ generated by the flexoelectric polarization [42], thus no electro-optical signal could be detected at usual (a few ten volts) AC applied voltages.

In a homeotropic sample, an in-plane electric field may induce director distortions only *via* the converse flexoelectric effect (Helfrich-geometry [35]). Such an electro-optical response has been measured for **ClPbis10BB**; from that $e_3 \approx 20$ pC m^{-1} was deduced [50], which is in the order of e_3 of a calamitic nematic. As the finite value of the anchoring strength has not been taken into account at calculating e_3, the above value can be regarded as a lower limit. Even then the value is much lower than the giant one obtained by flexing measurements.

The giant e_3 obtained by flexing of **ClPbis10BB** is significantly larger than that predicted by the molecular statistical models [35–37] which regard each molecule as an individually rotating/fluctuating unit. This implies that in BC nematics there must be a collective contribution to flexoelectricity coming from a group (cluster) of molecules.

Indeed, the bent molecular shape favors a short-range polar ordering (association of the molecules forming clusters) as indicated by several other types of measurements [16,28,30]. The polar cluster contribution seems to need an activation either by strong mechanical deformations (bending of flexible substrates, or director gradient in a HAN cell) or a threshold electric voltage (converse giant flexoelectricity); remaining below the threshold (which occurred in the experiment utilizing the Helfrich-geometry) the collective contribution is invisible and from flexoelectric point of view the BC nematic behaves just as a calamitic one, explaining why no large flexoelectricity was observed in those experiments.

6. Small angle X-ray measurements: nanostructure

SAXS from the uniaxial nematic phase of **ClPbis10BB** is shown to be consistent with the presence of molecular clusters possessing short-range tilted smectic (smectic-C) order [51]. SAXS studies of isotropic, nematic, and smectic mesophases formed in the binary mixtures of **ClPbis10BB** and the rod-shaped **6OO8** molecules were also reported [52]. While optical studies indicated [24] that the components are fully miscible, SAXS reveals fascinating structures that are consistent with segregation on a nanoscopic scale (Figure 5). It was found that the tilted smectic clusters reported by Hong et al. [51], in both the nematic and isotropic states of the pure **ClPbis10BB**, are also present in mixtures with up to 50 wt% of the **6OO8** compound; this is consistent with previous dielectric and flexoelectric studies on such mixtures. Unexpectedly in this concentration range, the clusters are present in the isotropic and in the induced smectic phase range, as well as throughout the nematic phase.

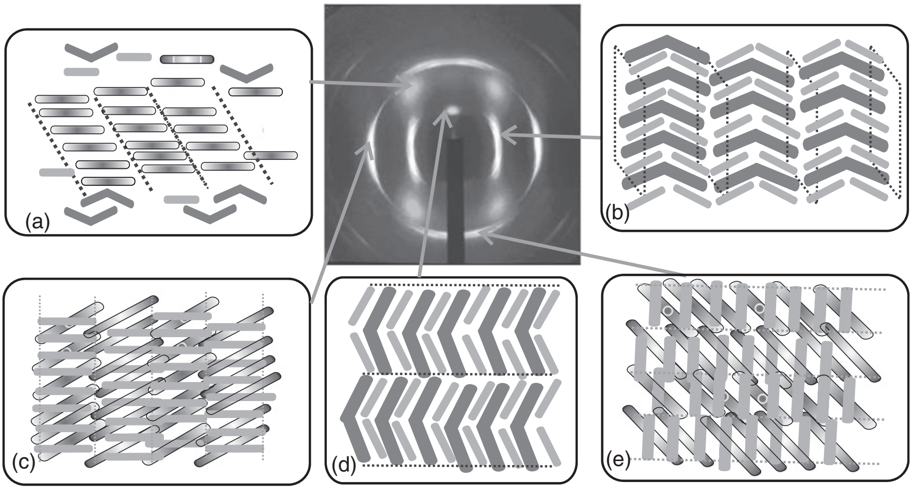

Figure 5. Representative 2D SAXS patterns and their corresponding proposed cartoons of the nanostructures in the smectic phase 5°C above the crystal transition of 17 wt% **6OO8** – 83 wt% **ClPbis10BB** mixture. Dotted lines indicate the layering. A thicker dotted line indicates a shorter correlation length. (a) Smectic clusters, (b) smectic layers normal to the magnetic field with periodicity corresponding to the length of the BC molecules, (c) smectic layers normal to the magnetic field with periodicity corresponding to the periodicity of the rod-shape molecules, (d) smectic layers parallel to the magnetic field with periodicity corresponding to the length of the BC molecules and (e) smectic layers parallel to the magnetic field with periodicity corresponding to the periodicity of the rod-shape molecules.

The results in the smectic phase also reveal complex layering phenomena, providing important insight into the interaction between bent and rod-shaped molecules. These studies will be crucial in the design of promising new functional nano-materials.

7. Elastic and rheological properties

The rotational viscosity was measured by analyzing the dynamics of the director rotation in pulsed magnetic fields, and the flow viscosities were determined by employing a new electro-rotation technique [53]. The results show that whereas the rotational viscosity is more than 10 times larger than for calamitic LCs, the flow viscosity is more than 100 times larger. Even more striking is the difference between the ratio of the flow and rotational viscosities, which for calamitic nematics is typically 0.1, whereas in **ClPbis10BB** it is 50. This suggests that the large shear viscosity is primarily due not so much to the molecular size, but rather to the shape, which leads to smectic clusters that make the material sticky.

It was also shown that **ClPbis10BB** exhibits non-Newtonian flow even in its optically isotropic liquid phase as shown in Figure 6 [54]. This behavior is also due to the existence of nanostructured, fluctuating clusters composed of a few smectic-like layers. Shear alignment of these clusters explains the shear thinning observed in **ClPbis10BB** in the nematic and optically isotropic phases.

Using DLS and Freedericksz-transitions induced in applied magnetic and electric fields, the absolute magnitudes of the Frank elastic constants and effective orientational viscosities of **ClPbis10BB** have been determined [29]. At a fixed temperature, 2°C below

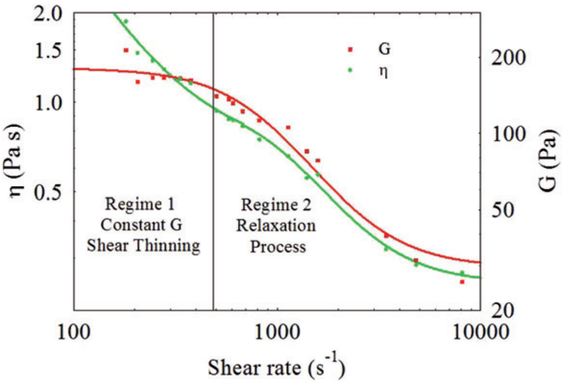

Figure 6. The viscoelastic response of **ClPbis10BB** over two decades of shear rates. We see the presence of two regimes. The first has a constant shear modulus and a shear thinning viscosity, while the second is characterized by a strong relaxation process for both the properties. This suggests that the first regime is probably dominated by permeation while the second shows the effects of shear alignment of the aggregates.

the isotropic-nematic transition, it was found that $K_{11} = 3.1\,\mathrm{pN}$, $K_{22} = 0.31\,\mathrm{pN}$, $K_{33} = 0.88\,\mathrm{pN}$, $\eta_{\mathrm{splay}} = 1.1\,\mathrm{Pas}$, $\eta_{\mathrm{twist}} = 0.37\,\mathrm{Pas}$, and $\eta_{\mathrm{bend}} = 1.2\,\mathrm{Pas}$. The unusual anisotropies of these parameters ($K_{33} < K_{11}$ and $K_{22} \ll K_{11}$) were explained in terms of short-range, smectic-C-like correlations among molecules in the nematic phase.

8. Electric field induced patterns

Excitation of a nematic by an electric field often triggers a pattern forming instability involving (usually spatially periodic) deformation of the director field, which is typically associated with material flow. Depending on the material parameters (primarily on ε_a and σ_a) and the cell geometry (planar or homeotropic) [55] electroconvection (EC) patterns exhibit a great richness in morphology [56,57]. They are often characterized by a sequence of dark and bright stripes when viewed in a polarizing microscope. Electroconvective stripe patterns were detected also in **ClPbis10BB** when testing a planar cell (with thickness $d = 15\,\mu\mathrm{m}$) at $T = 75°\mathrm{C}$ [16]. The studied frequency range of $10\,\mathrm{Hz} \leq f \leq 100\,\mathrm{kHz}$ comprises four morphological regions. As examples Figure 7 shows snapshots of typical EC patterns. A common feature of all patterns seen in **ClPbis10BB** is that each is visible with crossed (or nearly crossed) polarizers only, they do not produce a shadowgraph image.

For $f \leq 28\,\mathrm{Hz}$ stripes running nearly parallel to the initial director (PS, Figure 7) were seen with a wavelength about the sample thickness d. PS patterns are typically not well ordered, they break into smaller domains. The threshold voltage of the pattern increases linearly with the excitation frequency as shown in Figure 8(a). These features imply that the PS pattern may be identified as non-standard EC similar to those seen in calamitic nematics with $\varepsilon_a < 0$ and $\sigma_a < 0$. We note that a similar pattern observed by Le et al. [50] was interpreted as flexoelectric domains (i.e., static deformation without flow); the **ClPbis10BB** batch used by them had, however, much lower conductivity. As flexoelectricity provides the driving mechanism for both flexoelectric domains and non-standard EC, moreover a higher conductivity usually favors flow, the difference in the explanation of the patterns is understandable.

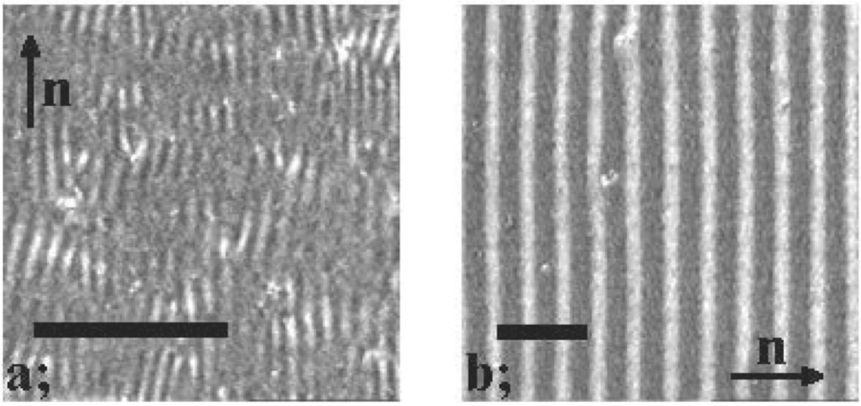

Figure 7. Snapshots of EC patterns in a 15 μm planar cell of **ClPbis10BB** at 75°C taken at crossed polarizers. (a) PS at 12 Hz, 28 V(rms), (b) wide stripes (PW2) at 200 Hz, 48 V(rms). The black bar denotes a distance of 100 μm; the arrows mark the rubbing direction (**n**).

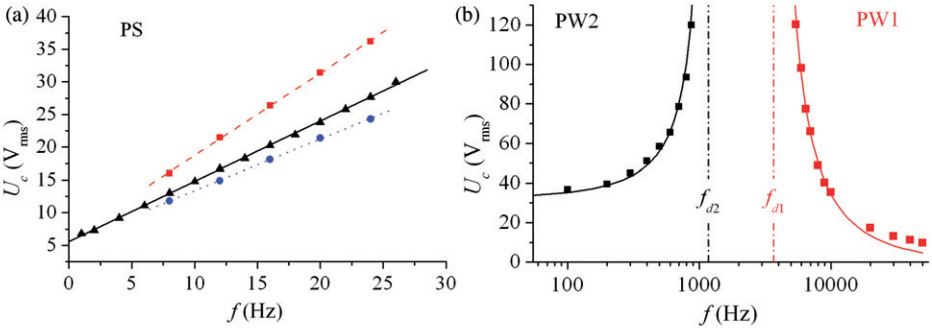

Figure 8. Frequency dependence of the threshold voltages of EC patterns in **ClPbis10BB**. (a) PS at 70°C (squares), 75°C (triangles), and 77°C (circles). The straight lines are linear fits. (b) Wide stripes (PW1 and PW2) at 75°C. Solid lines are hyperbolic fits; dash-dotted lines mark the divergence frequencies.

At higher frequencies wide stripes oriented normal to **n** (Figure 8b) were observed except in a frequency gap (1 kHz $< f <$ 5 kHz), where no pattern arose at all. The patterns PW2 and PW1 at the lower and higher f side of the frequency gap, respectively, have very similar characteristics; they are practically undistinguishable by their optical appearance. The patterns are well ordered; their wavelength is approximately about $3d$. They are reminiscent of the prewavy pattern reported for calamitic nematics [58–61]. The growth and decay of the pattern is extremely slow, it occurs on the time scale of hours. The main difference between PW2 and PW1 lies in their $U_c(f)$ dependence depicted in Figure 8(b); both exhibit a hyperbolic divergence of the onset voltage [$U_c \propto (f_{d2} - f)^{-1}$ at $f \to f_{d2}$ and $U_c \propto (f - f_{d1})^{-1}$ at $f \to f_{d1}$], though approaching the divergence frequencies, f_{d2} and f_{d1} respectively, from the opposite direction. This behavior of **ClPbis10BB** is unprecedented. To our knowledge, EC has not yet been observed at frequencies near to 100 kHz, moreover, neither experimental data have indicated nor any theoretical models have predicted a negative slope of the $U_c(f)$ curve for calamitic nematics; similar behavior has, however, been observed in other BC nematics [62].

EC scenarios were also studied in binary mixtures of **ClPbis10BB** with **6OO8** [63]. It was found that at low (~30 wt%) calamitic concentration the banana-specific peculiarities qualitatively persist. The higher **6OO8** content mostly affects the high f scenarios with $dU_c/df < 0$ resulting in morphological changes and in disappearing of that branch for ≥ 70 wt% of **6OO8**.

9. Conclusions

We have shown that the BC **ClPbis10BB** has a large number of unusual physical properties. Its bend flexoelectric coefficient is 1000 times larger than in calamitics; it is viscoelastic with a large shear rate dependent viscosity. Its bend and twist elastic constants are abnormally low and the nematic phase can be rendered to be a blue fog phase with a small amount of chiral dopant. It shows a record high flow birefringence and very small leading Landau coefficient. It has two types of isotropic phase; the lower temperature one probably is a tetrahedratic phase that can be transferred to the nematic phase with a relatively low magnetic field. **ClPbis10BB** also has a frequency-dependent conductivity anisotropy which is characterized by a double sign inversion and exhibits unusual EC scenarios depending on the frequency of the applied voltage. We find that all these abnormal properties are due to the presence of smectic clusters in its isotropic and nematic phases that could be clearly observed by SAXS measurements. The proposed nanostructure of **ClPbis10BB** in the nematic phase is depicted in Figure 9. Measurements show that

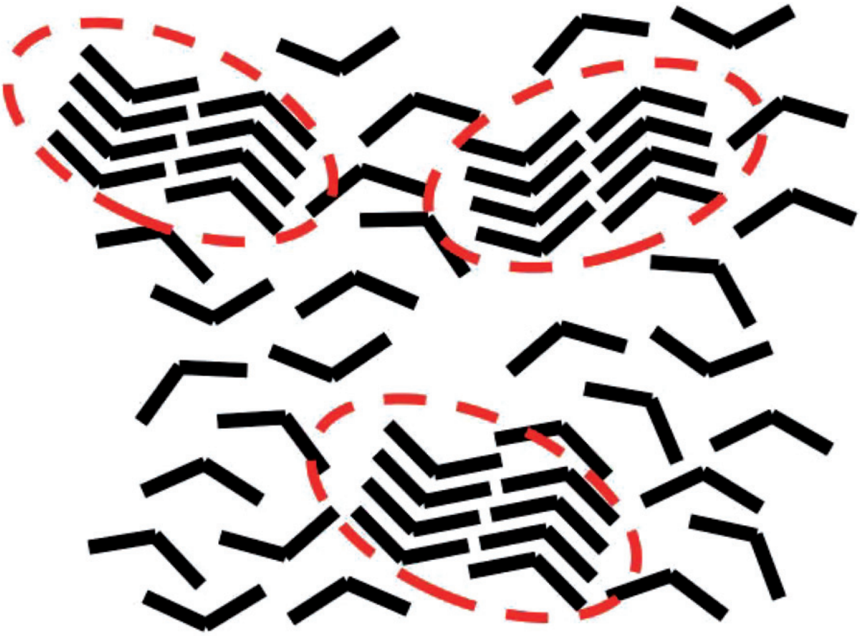

Figure 9. Proposed nanostructure of the material **ClPbis10BB** in the nematic phase based on all the experiments summarized in this article. The smectic clusters have sizes in the 20–40 nm range, and the director in the smectic clusters is tilted by about 45°, and they should at least partially be ferroelectric.

smectic clusters have sizes in the 20–40 nm range, and the director in the smectic clusters is tilted by about 45°, and they should at least partially be ferroelectric.

Acknowledgments

Financial supports by the Hungarian Research Funds OTKA-K-81250 and by NSF DMR-0964765 are gratefully acknowledged.

References

[1] H. Takezoe and Y. Takanishi, *Bent-core liquid crystals: Their mysterious and attractive world*, Jpn. J. Appl. Phys. 45 (2006), pp. 597–625.

[2] G. Pelzl, S. Diele, and W. Weissflog, *Banana-shaped compounds – A new field of liquid crystals*, Adv. Mater. 11 (1999), pp. 707–724.

[3] T. Niori, T. Sekine, J. Watanabe, T. Furukawa, and H. Takezoe, *Distinct ferroelectric smectic liquid crystals consisting of banana shaped achiral molecules*, J. Mater. Chem. 6 (1996), pp. 1231–1233.

[4] T. Sekine, T. Niori, M. Sone, J. Watanabe, S.W. Choi, Y. Takanishi, and H. Takezoe, *Origin of helix in achiral banana-shaped molecular systems*, Jpn. J. Appl. Phys. 36 (1997), pp. 6455–6463.

[5] H.R. Brand, P.E. Cladis, and H. Pleiner, *Polar biaxial liquid crystalline phases with fluidity in two and three spatial dimensions*, Int. J. Eng. Sci. 38 (2000), pp. 1099–1112.

[6] B. Mettout, P. Toledano, H. Takezoe, and J. Watanabe, *Theory of polar biaxial nematic phases*, Phys. Rev. E 66 (2002), p. 031701.

[7] T.C. Lubensky and L. Radzihovsky, *Theory of bent-core liquid-crystal phases and phase transitions*, Phys. Rev. E 66 (2002), p. 031704.

[8] L. Radzihovsky and T.C. Lubensky, *Fluctuation-driven 1st-order isotropic-to-tetrahedratic phase transition*, Europhys. Lett. 54 (2001), pp. 206–212.

[9] I. Dozov, *On the spontaneous symmetry breaking in the mesophases of achiral banana-shaped molecules*, Europhys. Lett. 56 (2001), pp. 247–253.

[10] J. Matraszek, J. Mieczkowski, J. Szydlowska, and E. Gorecka, *Nematic phase formed by banana-shaped molecules*, Liq. Cryst. 27 (2000), pp. 429–436.

[11] I. Wirth, S. Diele, A. Eremin, G. Pelzl, S. Grande, L. Kovalenko, N. Pancenko, and W. Weissflog, *New variants of polymorphism in banana-shaped mesogens with cyano-substituted central core*, J. Mater. Chem. 11 (2001), pp. 1642–1650.

[12] W. Weissflog, H. Nádasi, U. Dunemann, G. Pelzl, S. Diele, A. Eremin, and H. Kresse, *Influence of lateral substituents on the mesophase behaviour of banana-shaped mesogens*, J. Mater. Chem. 11 (2001), pp. 2748–2758.

[13] E. Mátyus and K. Keserü, *Synthesis, characterization and theoretical considerations of a novel class of banana-shaped compounds with liquid crystal properties*, J. Mol. Struct. 543 (2001), pp. 89–98.

[14] T.J. Dingemans and E.T. Samulski, *Non-linear boomerang-shaped liquid crystals derived from 2,5-bis(p-hydroxyphenyl)-1,3,4-oxadiazole*, Liq. Cryst. 27 (2000), pp. 131–136.

[15] K. Fodor-Csorba, A. Vajda, G. Galli, A. Jákli, D. Demus, S. Holly, and E. Gács-Baitz, *Ester-type banana-shaped monomers and investigations of their electro-optical properties*, Macromol. Chem. Phys. 203 (2002), pp. 1556–1563.

[16] D. Wiant, J.T. Gleeson, N. Éber, K. Fodor-Csorba, A. Jákli, and T. Tóth-Katona, *Nonstandard electroconvection in a bent-core nematic liquid crystal*, Phys. Rev. E 72 (2005), p. 041712.

[17] D. Wiant, S. Stojadinovic, K. Neupane, S. Sharma, K. Fodor-Csorba, A. Jákli, J.T. Gleeson, and S. Sprunt, *Critical behavior at the isotropic-to-nematic phase transition in a bent-core liquid crystal*, Phys. Rev. E 73 (2006), p. 030703(R).

[18] J. Harden, B. Mbanga, N. Éber, K. Fodor-Csorba, S. Sprunt, J.T. Gleeson, and A. Jákli, *Giant flexoelectricity of bent-core nematic liquid crystals*, Phys. Rev. Lett. 97 (2006), p. 157802.

[19] D. Wiant, K. Neupane, S. Sharma, A. Jákli, J.T. Gleeson, and S. Sprunt, *Observation of a possible tetrahedratic phase in bent-core liquid crystals*, Phys. Rev. E 77 (2008), p. 061701.

[20] H.R. Brand, H. Pleiner, and P.E. Cladis, *Tetrahedratic cross-couplings: Novel physics for banana liquid crystals*, Physica A 351 (2005), pp. 189–197.

[21] T. Ostapenko, D.B. Wiant, S.N. Sprunt, A. Jákli, and J.T. Gleeson, *Magnetic-field induced isotropic to nematic liquid crystal phase transition*, Phys. Rev. Lett. 101 (2008), p. 247801.

[22] C. Bailey, K. Fodor-Csorba, R. Verduzco, J.T. Gleeson, S. Sprunt, and A. Jákli, *Large flow-birefringence of nematogenic bent-core liquid crystals*, Phys. Rev. Lett. 103 (2009), p. 237803.

[23] J.P. van Meter and B.H. Klanderman, *Mesomorphic properties of some phenyl benzoate derivatives*, Mol. Cryst. Liq. Cryst. 22 (1973), pp. 271–284.

[24] G.G. Nair, C.A. Bailey, S. Taushanoff, K. Fodor-Csorba, A. Vajda, Z. Varga, A. Bóta, and A. Jákli, *Electrically tunable color using mixtures of bent-core and rod-shape molecules*, Adv. Mater. 20 (2008), pp. 3138–3142.

[25] P.P. Crooker, *Blue phases*, in *Chirality in Liquid Crystals*, H.-S. Kitzerow and C. Bahr, eds., Springer-Verlag, New York, 2004, pp. 186–222.

[26] S. Taushanoff, K.V. Le, J. Williams, R.J. Twieg, B.K. Sadashiva, H. Takezoe, and A. Jákli, *Stable amorphous blue phase of bent-core nematic liquid crystals doped with a chiral material*, J. Mater. Chem. 20 (2010), pp. 5893–5898.

[27] L. Calucci, C. Forte, K. Fodor-Csorba, B. Mennucci, and S. Pizzanelli, *Conformations of banana-shaped molecules studied by H-2 NMR spectroscopy in liquid crystalline solvents*, J. Phys. Chem. B 111 (2007), pp. 53–61.

[28] V. Domenici, C.A. Veracini, and B. Zalar, *How do banana-shaped molecules get oriented (if they do) in the magnetic field?*, Soft Matter 1 (2005), pp. 408–411.

[29] M. Majumdar, P. Salamon, A. Jákli, J.T. Gleeson, and S. Sprunt, *Elastic constants and orientational viscosities of a bent-core nematic liquid crystal*, Phys. Rev. E 83 (2011), p. 031701.

[30] V. Domenici, K. Fodor-Csorba, D. Frezzato, G. Moro, and C.A. Veracini, *Deuterium NMR evidences of slow dynamics in the nematic phase of a banana-shaped liquid crystal*, Ferroelectrics 344 (2006), pp. 263–272.

[31] V. Domenici, C.A. Veracini, K. Fodor-Csorba, G. Prampolini, I. Cacelli, A. Lebar, and B. Zalar, *Banana-shaped molecules peculiarly oriented in a magnetic field: H-2 NMR spectroscopy and quantum mechanical calculations*, Chem. Phys. Chem. 8 (2007), pp. 2321–2330.

[32] P. Salamon, N. Éber, Á. Buka, J.T. Gleeson, S. Sprunt, and A. Jákli, *Dielectric properties of mixtures of a bent-core and a calamitic liquid crystal*, Phys. Rev. E 81 (2010), p. 031711.

[33] R.B. Meyer, *Piezoelectric effects in liquid crystals*, Phys. Rev. Lett. 22 (1969), pp. 918–921.

[34] P.G. de Gennes and J. Prost, *The Physics of Liquid Crystals*, Clarendon Press, Oxford, 1993.

[35] W. Helfrich, *A simple method to observe the piezoelectricity of liquid crystals*, Phys. Lett. 35A (1971), pp. 393–394.

[36] W. Helfrich, *The strength of piezoelectricity in liquid crystals*, Z. Naturforsch. 26a (1971), pp. 833–835.

[37] A. Derzhanski and A.G. Petrov, *A molecular-statistical approach to the piezoelectric properties of nematic liquid crystals*, Phys. Lett. 36A (1971), pp. 483–484.

[38] P.R. Mahesware Murthy, V.A. Ragunathan, and N.V. Madhusudana, *Experimental determination of the flexoelectric coefficients of some nematic liquid crystals*, Liq. Cryst. 14 (1993), pp. 483–496.

[39] L.A. Beresnev, L.M. Blinov, S.A. Davidyan, S.G. Konov, and S.B. Yablonskii, *Direct measurement of the flexoelectric polarization of nematic liquid-crystals*, JETP Lett. 45 (1987), pp. 755–758.

[40] J. Harden, R. Teeling, J.T. Gleeson, S. Sprunt, and A. Jákli, *Converse flexoelectric effect in a bent-core nematic liquid crystal*, Phys. Rev. E 78 (2008), p. 031702.

[41] A. Jákli, M. Chambers, J. Harden, M. Madhabi, R. Teeling, J. Kim, Q. Li, G.G. Nair, N. Éber, K. Fodor-Csorba, J.T. Gleeson, and S. Sprunt, *Extraordinary properties of nematic phases of bent-core liquid crystals*, Proceedings of SPIE on Emerging Liquid Crystal Technologies III, Vol. 6911, San Jose, 20–24 January, USA, 2008, p. 691105.

[42] G. Barbero, P.T. Valabrega, R. Bartolino, and B. Valenti, *Evidence for the flexo-electric effect in a nematic liquid crystal cell*, Liq. Cryst. 1 (1986), pp. 483–490.

[43] B. Valenti, C. Bertoni, G. Barbero, P. Taverna Valabrega, and R. Bartolino, *Flexoelectricity in the hybrid aligned nematic cell*, Mol. Cryst. Liq. Cryst. 146 (1987), pp. 307–320.

[44] I. Dozov, Ph. Martinot-Lagarde, and G. Durand, *Flexoelectrically controlled twist of texture in a nematic liquid-crystal*, J. Phys. Lett. 43 (1982), pp. 365–369.

[45] S. Warrier and N.V. Madhusudana, *An AC electrooptic technique for measuring the flexoelectric coefficient* $(e(1)+e(3))$ *and anchoring energies of nematics*, J. Phys. II 7 (1997), pp. 1789–1803.

[46] L.M. Blinov, M.I. Barnik, H. Ohoka, M. Ozaki, and K. Yoshino, *Separate measurements of the flexoelectric and surface polarization in a model nematic liquid crystal p-methoxybenzylidene-p'-butylaniline: Validity of the quadrupolar approach*, Phys. Rev. E 64 (2001), p. 031707.

[47] N.T. Kirkman, T. Stirner, and W.E. Hagston, *Continuum modelling of hybrid-aligned nematic liquid crystal cells: Optical response and flexoelectricity-induced voltage shift*, Liq. Cryst. 30 (2003), pp. 1115–1122.

[48] S. Ponti, P. Ziherl, C. Ferrero, and S. Zumer, *Flexoelectro-optic effect in a hybrid nematic liquid crystal cell*, Liq. Cryst. 26 (1999), pp. 1171–1177.

[49] T. Takahashi, S. Hashidate, H. Nishijou, M. Usui, M. Kimura, and T. Akahane, *Novel measurement method for flexoelectric coefficients of nematic liquid crystals*, Jpn. J. Appl. Phys. 37 (1998), pp. 1865–1869.

[50] K.V. Le, F. Araoka, K. Fodor-Csorba, K. Ishikawa, and H. Takezoe, *Flexoelectric effect in a bent-core mesogen*, Liq. Cryst. 36 (2009), pp. 1119–1124.

[51] S.H. Hong, R. Verduzco, J. Williams, R.J. Twieg, E. DiMasi, R. Pindak, A. Jákli, J.T. Gleeson, and S. Sprunt, *Short range smectic order in bent-core nematic liquid crystals*, Soft Matter 6 (2010), pp. 4819–4827.

[52] S.H. Hong, R. Verduzco, J.T. Gleeson, S. Sprunt, and A. Jákli, *Nanostructures of liquid crystal phases in mixtures of bent core and rod-shaped molecules*, Phys. Rev. E. 83 (2011), p. 061702.

[53] E. Dorjgotov, K. Fodor-Csorba, J.T. Gleeson, S. Sprunt, and A. Jákli, *Viscosities of a bent-core nematic liquid crystal*, Liq. Cryst. 35 (2008), pp. 149–155.

[54] C. Bailey, K. Fodor-Csorba, J.T. Gleeson, S.N. Sprunt, and A. Jákli, *Rheological properties of bent-core liquid crystals*, Soft Matter 5 (2009), pp. 3618–3622.

[55] Á. Buka, N. Éber, W. Pesch, and L. Kramer, *Convective patterns in liquid crystals driven by electric field*, in *Self-Assembly, Pattern Formation and Growth Phenomena in Nano-systems*, Vol. 218, A.A. Golovin and A.A. Nepomnyashchy, eds., Springer, Dordrecht, 2006, pp. 55–82 [NATO Science Series II, Mathematica, Physics and Chemistry].

[56] L.M. Blinov and V.G. Chigrinov, *Electrooptic Effects in Liquid Crystal Materials*, Springer, New York, 1994.

[57] L. Kramer and W. Pesch, *Electrohydrodynamic instabilities in nematic liquid crystals*, in *Pattern Formation in Liquid Crystals*, Á. Buka and L. Kramer, eds., Springer, New York, 1996, pp. 221–256.

[58] P. Petrescu and M. Giurgea, *A new type of domain structure in nematic liquid crystals*, Phys. Lett. 59A (1976), pp. 41–42.

[59] A.N. Trufanov, M.I. Barnik, and L.M. Blinov, *A novel type of electrohydrodynamic instability in nematic liquid crystals*, in *Advances in Liquid Crystal Research and Applications*, L. Bata, ed., Akadémiai Kiadó, Pergamon Press, Budapest, New York, 1980, pp. 549–560.

[60] L. Nasta and A. Lupu, *Characteristics of domains appearing in nematic liquid-crystals below the threshold voltage of chevrons*, Mol. Cryst. Liq. Cryst. 71 (1981), pp. 65–76.

[61] J-H. Huh, Y. Hidaka, Y. Yusuf, N. Éber, T. Tóth-Katona, Á. Buka, and S. Kai, *Prewavy pattern: A director-modulation structure in nematic liquid crystals*, Mol. Cryst. Liq. Cryst. 364 (2001), pp. 111–122.

[62] P. Tadapatri, U.S. Hiremath, C.V. Yelamaggad, and K.S. Krishnamurthy, *Patterned electroconvective states in a bent-core nematic liquid crystal*, J. Phys. Chem. B 114 (2010), pp. 10–21.

[63] S. Tanaka, H. Takezoe, N. Éber, K. Fodor-Csorba, A. Vajda, and Á. Buka, *Electroconvection in nematic mixtures of bent-core and calamitic molecules*, Phys. Rev. E 80 (2009), p. 021702.